Computers and Concrete, *Vol. 23, No. 1 (2019) 49-60*
DOI: https://doi.org/10.12989/cac.2019.23.1.049

Determining the shear strength of FRP-RC beams using soft computing and code methods

Gunnur Yavuz*

Department of Civil Engineering, Faculty of Engineering and Natural Sciences, Konya Technical University, Konya, Turkey

(Received April 9, 2018, Revised January 17, 2019, Accepted January 22, 2019)

Abstract. In recent years, multiple experimental studies have been performed on using fiber reinforced polymer (FRP) bars in reinforced concrete (RC) structural members. FRP bars provide a new type of reinforcement that avoids the corrosion of traditional steel reinforcement. In this study, predicting the shear strength of RC beams with FRP longitudinal bars using artificial neural networks (ANNs) is investigated as a different approach from the current specific codes. An ANN model was developed using the experimental data of 104 FRP-RC specimens from an existing database in the literature. Seven different input parameters affecting the shear strength of FRP bar reinforced RC beams were selected to create the ANN structure. The most convenient ANN algorithm was determined as traingdx. The results from current codes (ACI440.1R-15 and JSCE) and existing literature in predicting the shear strength of FRP-RC beams were investigated using the identical test data. The study shows that the ANN model produces acceptable predictions for the ultimate shear strength of FRP-RC beams (maximum $R^2 \approx 0.97$). Additionally, the ANN model provides more accurate predictions for the shear capacity than the other computed methods in the ACI440.1R-15, JSCE codes and existing literature for considering different performance parameters.

Keywords: internal FRP bar; reinforced concrete; beam; shear strength; artificial neural network

1. Introduction

Fiber reinforced polymer (FRP) bars have a higher structural strength to weight ratio and excellent corrosion resistance when compared to steel bars. Therefore, FRP bars can be used as reinforcement instead of the traditional steel reinforcement (Rizkalla *et al*. 2003). Reinforcement steel corrosion occurs under various environmental conditions such as air pollution and high moisture. Steel bar corrosion is an important problem in the construction industry. Concrete can be damaged because of the corrosion of the steel reinforcement in reinforced concrete structural members. Because of this damage in concrete, time-consuming and expensive rehabilitation procedures may need to be applied. FRP reinforcements are more expensive than traditional steel reinforcements, but these reinforcements have potential savings in maintenance and repair costs. Therefore, FRP bars can be used as an alternative to other reinforcements (Bank and Shapira 1997). Another feature of FRP reinforcements is the easy monitoring of structural members with remote sensing. Smart structures can be built by using sensors placed on FRP reinforcements, allowing structural health monitoring. This combination can be used in deformed reinforcement bars, two and three dimensional grid reinforcements and prestressing tendons. In recent years, experimental and theoretical investigations have been performed on using FRP composites as reinforcement in concrete and masonry structures and standardizing the design methods for structural members that are internally reinforced or externally rehabilitated by FRP materials (Bousselham and Chaallal 2006, Costa and Barros 2010, Ju *et al*. 2017). The commonly available FRP materials in reinforcing, repairing and strengthening are glass (GFRP), aramid (AFRP), carbon (CFRP) and basalt (BFRP).

A lot of experimental studies have been performed on FRP reinforced concrete (Duranovic *et al*. 1997, Tureyen and Frosch 2002, Tariq and Newhook 2003, Gross *et al*. 2004). As a result of these previous studies, current codes for FRP reinforced concrete members were developed. A large number of codes cover FRP reinforced concrete such as ACI 440.1R-15 (2015), CSA-S806-02 (2007), CNR-DT 203/2006 (2007), *fib* Bulletin No. 40 (2007), ISIS Design Manual No. 3 (2007) and JSCE (1997).

Artificial neural networks (ANNs) are an artificial intelligence application implemented by engineers, notably to perform design tasks since the 1980s. ANNs are applied to perform many different tasks including the prediction of function, approximation, classification, and filtering (Arslan 2010). ANNs have been successfully applied to a number of areas in civil engineering applications. Studies have investigated structural analysis and design, structural damage assessment, evaluation of earthquake performance of reinforced concrete structures, estimation of water levels in lakes, and predictions of stream flow (Hadi 2003, Yavuz *et al*. 2015, Yavuz 2016, Inel 2007, Elkordy 1993, Lautour and Omenzetter 2009, Buyukyildiz *et al*. 2014, Arslan 2013).

The aims of this study are to examine the performance of ANN models when predicting the shear strength of RC beams reinforced with internal FRP bars and to evaluate the

*Corresponding author, Ph.D.
E-mail: gyavuz@ktun.edu.tr

http://www.techno-press.org/?journal=cac&subpage=8 ISSN: 1598-8198 (Print), 1598-818X (Online)

Table 1 Shear strength formulas related to the different design codes and EL for FRP-RC beams

Code	Shear strength. V_c
ACI 440-1R-15 (2015)	$V_{cf}=\left(\frac{5}{2}k\right)2\sqrt{f_c^{'}}b_w d$ or $V_{cf}=\frac{2\sqrt{f_c^{'}}}{5}.b_w.c$, $c=kd$. $k=\sqrt{2\rho_f n_f+(\rho_f n_f)^2}-\rho_f n_f$. $\rho_f=\frac{A_f}{b_w d}$, $n_f=\frac{E_f}{E_c}$
JSCE (1997)	$V_{cf}=0.2.\sqrt[4]{1000/d}.\sqrt[3]{100.\frac{A_f}{b_w.d}.\frac{E_f}{E_s}}\sqrt[3]{f_c^{'}}.b_w.d$
EL (Kara 2011)	$V_{cf}=b_w d(\sqrt[5]{\frac{d}{a}f_c'\rho_f\frac{E_f}{E_s}}(\frac{c_1^2}{c_0})^2)^{1/3}(c_0/c_2)$ c_o=7.696, c_1=7.254 and c_2=7.718.

accuracy of the applicable codes in predicting the shear capacity of these types of RC beams. To achieve these goals, experimental data for 104 RC beams and one-way slabs (91 beams and 13 one-way slabs) were selected from the existing database in the previous study by Kara (2011). Using their experimental results, the back-propagation algorithm was performed to train for the shear strength of RC beams which were reinforced with internal FRP bars. The training error, test error, and correlation coefficient (R^2) indicating the initial performance evaluation of the back propagation was also compared. Furthermore, the results of selected building codes and existing literature methods are also examined by comparing their predictions with the data from the experimental studies. The results obtained by the ANN, code approaches and existing literature methods are compared.

2. Design methods according to the codes (ACI440.1R-15, JSCE) and Existing Literature (EL)

The design of FRP-reinforced concrete is similar to that of steel-reinforced concrete members. However, the different mechanical properties of FRP bars (such as the relatively low modulus of elasticity, low transverse shear resistance, high tensile strength and absent yield point) affect the shear strength and must be considered (ACI440.1-R-15 2015). The shear strength formulas related to different design codes and existing literature (EL) for FRP-RC beams are listed in Table 1.

2.1 ACI440.1R-15 code

In this code, the contribution of longitudinal FRP reinforcement in terms of dowel action has not been determined because of the lower strength and stiffness of FRP bars in the transverse direction. ACI 440.1R-15 adopted the beam shear model from Tureyen and Frosch (2003). The concrete shear capacity V_c, of flexural members using FRP as the main reinforcement can be evaluated according to Eq. (1) in SI units according to ACI440.1R-15 code (2015).

$$V_c=\frac{2}{5}\sqrt{f_c^{'}}b_w c \tag{1}$$

where b_w is the width of the beam web (mm) and c is the cracked transformed section neutral axis depth (mm). For singly reinforced, rectangular cross sections, the neutral axis depth, c, may be computed by Eq. (2).

$$c=kd \tag{2}$$

$$k=\sqrt{2\rho_f n_f+(\rho_f n_f)^2}-\rho_f n_f \tag{3}$$

$$\rho_f=\frac{A_f}{b_w d} \tag{4}$$

In Eq. (4), ρ_f is the longitudinal FRP reinforcement ratio. Eq. (1) accounts for the axial stiffness of the FRP reinforcement through the neutral axis depth c, which is a function of the reinforcement ratio, ρ_f, and the modular ratio, n_f. According to ACI440.1R-15, Eq. (1) may be rewritten as follows; in this equation, the axial stiffness of the FRP reinforcement is considered.

$$V_{cf}=\left(\frac{5}{2}k\right)2\sqrt{f_c^{'}}b_w d \tag{5}$$

2.2 JSCE code

The shear capacity of FRP-RC elements can be determined by Eq. (6) according to JCSE code (1997).

$$V_{cf}=0.2.\sqrt[4]{1000/d}.\sqrt[3]{100.\frac{A_f}{b_w.d}.\frac{E_f}{E_s}}\sqrt[3]{f_c^{'}}.b_w.d \tag{6}$$

In this equation, E_s is the steel elastic modulus (considered to be 200000 MPa), E_f is the FRP elastic modulus and $\sqrt[4]{1000/d}\le 1.5$, $.\sqrt[3]{100.(A_f/b_w.d).(E_f/E_s)}\le 1.5$, $V_{cf}=0.2\sqrt[3]{f_c^{'}}.\le 0.72$ limitations should be considered. $A_f/b_w.d$ represents the FRP reinforcement ratio, ρ.

2.3 Existing Literature (EL) proposed method

Kara (2011), proposed a new method for calculating V_{cf} for FRP-RC beams. In this study, a simple yet improved model presents to calculate the concrete shear strength of FRP-reinforced concrete slender beams (a/d>2.5) without stirrups based on the gene expression programming (GEP) approach. The proposed method accounts for the effect of well-known parameters on shear strength. The particular parameters include in training and testing of the GEP model, f_c', b_w, d, a/d, ρ_f and E_f/E_s were entered as input variables, while V_{cf} value was used as output variable. The shear resistance of a member V_{cf} is computed by Eq. (7) that is explicit formulation based on the GEP approach model according to Kara (2011).

$$V_{cf}=b_w d(\sqrt[5]{\frac{d}{a}f_c'\rho_f\frac{E_f}{E_s}}(\frac{c_1^2}{c_0})^2)^{1/3}(c_0/c_2) \tag{7}$$

In this equation, the constants are, c_o=7.696, c_1=7.254 and c_2=7.718.

3. Selection of the database

Multiple experimental data sets are available on the behavior of FRP-RC rectangular beams. The tests have been performed under similar loading types, and the selected parameters in these tests were similar. For instance, the parameters affecting the strength and ductility of FRP-RC beams were selected as the dimensions of the cross section, shear span to depth ratios, the compressive strength of concrete, the type of internal FRP (the FRP type was considered by the elastic modulus), the volumetric ratio of FRP internal reinforcement, and the mechanical properties of FRP reinforcement.

Information covering the basic data related to the beam geometry, the geometrical and mechanical material characteristics (the types of concrete and reinforcements), and the amount of the longitudinal reinforcements were required for the modeling process.

In this study, the examined specimens included 91 beams and 13 one-way slabs (totally 104 specimen), all were simply supported and were tested either in three-point or four point bending.

The *a/d* aspect ratio has a significant influence on the behavior of the reinforced concrete beams. In this study, the *a/d* aspect ratio was taken between 2.53-6.49. Additionally, shear span (aspect length) value varies between 600 and 1219.2 mm, and the effective depth, d, value varies between 141 and 360 mm.

The mechanical characteristics of the FRP bars used as reinforcement (such as tensile strength and elastic modulus) are among the major factors that govern the strength of a FRP-RC member. Therefore, in this study, different types of FRP internal reinforcement with different mechanical characteristics were considered during modeling. For instance, the modulus of elasticity of the FRP internal reinforcements varied over a wide range (32-145 GPa) in the beams.

When examining the equations in the current codes that cover the shear capacity of internal FRP-RC members, the compressive strength of concrete plays an important role in the efficiency of FRP. In this study, the range of the concrete compressive strength of the selected database varies between 24.1 and 81.4 MPa.

The volumetric ratio of the internal transverse reinforcement is also effective on the strength characteristics of RC beams; in this study, however, the selected beams from the EL database have no stirrups. The volumetric ratio of the longitudinal reinforcement of selected database varies between 0.0025 and 0.0302.

As explained above, the effect of the parameters on the behavior of FRP-RC beams were considered during the ANN modeling process. Therefore, the proposed model is valid for the majority of potential practical cases.

In this study, a total of 104 rectangular FRP-RC beam and one-way slab tests were collected from literature. The geometric and material properties of the specimens (Table Appendix) were taken from the study performed by Kara

Table 2 Range of parameters

Parameters	Identification	Range
b_w (mm)	width of beam	89-1000
a	shear span	600-1219.2
d	effective depth of beam	141-360
a/d	aspect ratio	2.53-6.49
f_c' (MPa)	cylindrical compressive strength of the concrete	24.1-81.4
E_f (GPa)	elasticity modulus of FRP	32-145
ρ_f (%)	longitudinal FRP reinforcement ratio	0.25-3.02

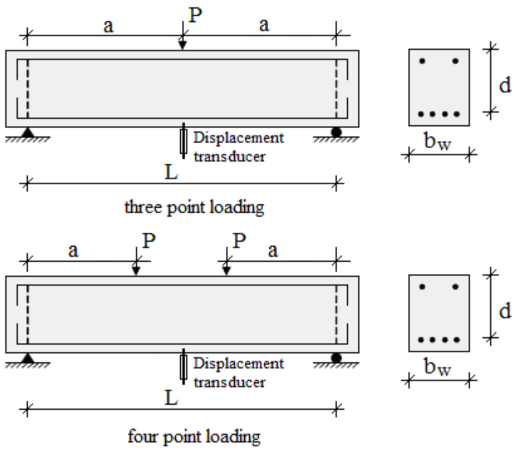

Fig. 1 Typical loading system and section of tested FRP-RC beams

(2011), which searched and documented other experimental studies (Duranovic *et al*. 1997, Tureyen and Frosch 2002, Tariq and Newhook 2003, Gross *et al*. 2004, Yost *et al*. 2001, El-Sayed *et al*. 2006, Razaqpur *et al*. 2004, Ashour 2006, El-Sayed *et al*. 2006, Gros *et al*. 2003, Alkhrdaji *et al*. 2001, Deitz *et al*. 1999, Mizukawa *et al*. 1997, Swamy and Aburawi 1997, Zhao *et al*. 1995). The experimental data for real-size type specimens consist of RC beams of rectangular cross-sections subjected to a shear load and flexure. In the reference study performed by Kara (2011), the performances of the shear strength of FRP-RC beam were examined by using the identical data in the literature. Kara (2011) improved and presented a gene expression programming (GEP) model to evaluate the shear resistance of FRP-RC slender beams without stirrups. The range of parameters covered by the considered specimens and a short description of the dataset is shown in Table 2. In Fig. 1, a typical testing setup is shown with the symbols used in the Table Appendix for the definition of the specimens.

4. Fundamental aspects of artificial neural network models

ANN models provide an alternative way to predict the shear strength of FRP-RC beams. A multilayer perceptron neural network (MLP-NN) is a feed-forward neural network model (Yavuz *et al*. 2014). The MLP model consists of one input layer, one or more hidden layers, and one output layer (Fu 1994). The structure of an ANN used in this study is

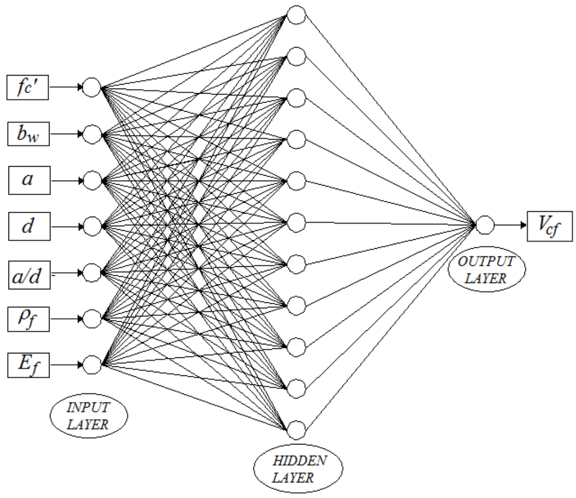

Fig. 2 ANN architecture of the selected model

given in Fig. 2. In the ANN model, the input parameters were selected based on the parameters affecting the shear strength of FRP-RC beams, which include the beam width (b_w), shear span (a), effective depth (d), aspect ratio (a/d), volumetric ratio of longitudinal FRP reinforcement (ρ_f), compressive concrete strength (f_c'), and elastic modulus of FRP reinforcement (E_f).

From Fig. 2, the general architecture of the feed-forward multilayer neural network with an error-back propagation model consists of one input layer having seven input nodes, one or more hidden layer(s) and one output layer having one output node. The neurons of a layer are fully connected to the neurons of neighboring layers with weights. The initial values of these weights are randomly assigned as small real values. In engineering problems, the number of input and output parameters is generally determined by design requirements. No general rule is available for selecting the number of neurons in a hidden layer; the number of hidden layer neurons is selected by the user and many trials are carried out to determine the most appropriate network models (Arslan 2010, Tezel and Buyukyildiz 2015). The neural network toolbox in MATLAB (2006) used in this study requires select parameters: the number of training data; the number of hidden layers; the number of iterations (epochs); the learning rate (l_r); the number of inputs, outputs and hidden nodes; the error tolerance and the momentum constant (m_c).

The back-propagation learning algorithm can be used to train the MLP network. Therefore, these weights are adjusted for a given set of input-output pairs (Rumelhart, 1986). In this study, ANNs were performed using a MATLAB software package (MATLAB version 7.11 with a neural networks toolbox). The input data were normalized in the range of [-1 1] and the output data were normalized in the range of [0 1]. Data scaling (normalization) is an important phase for network training. The input and output data are normalized before use in the network. Simple linear normalization functions were applied to the data by Eq. (8).

$$S_x = 2\frac{(X - X_{\min})}{(X_{\max} - X_{\min})} - 1 \qquad (\text{for } [-1\ 1])$$

$$S_x = \frac{(X - X_{\min})}{(X_{\max} - X_{\min})} \qquad (\text{for } [0\ 1]) \tag{8}$$

In Eq. (8), S_x is the normalized value of the variable X; $X_{\min}$ and $X_{\max}$ are the minimum and maximum values of X, respectively.

In this study, a hyperbolic tangent sigmoid transfer function was utilized on the hidden layer and the output layer. A training function, traingdx, was used to update the weight and bias values according to the gradient descent momentum and an adaptive learning rate. The performance of the network was sensitive to the learning rate (l_r). The learning rate was held constant throughout training for standard back-propagation. In the training process, the maximum training cycles, l_r, and m_c were selected to be 1000, 0.2 and 0.3, respectively. The ANN architecture consisted of seven input neurons including the geometrical and material properties of FRP-RC beams and one output neuron including the shear strength (Fig. 2). The number of neurons in the hidden layer varied from 10 to 100 to obtain the best results. The total data set contained 104×7 data-points. The data set was divided into equal training and testing data sets (52 data sets). The parameter combination that resulted in the best average training and testing performances was selected as the best for the suitable model. The optimum parameter combination is presented in Table 3. The study shows that the ANN model produces reasonable predictions of the shear strength of FRP-RC beams ($R^2 \approx 0.97$).

5. Comparison of existing design methods and the ANN model

5.1 The results of the ANN model

The database established by Kara (2011) was used in the ANN model; this database was comprised of 104 FRP-RC specimens that have been tested in various studies. The mean squared error (MSE %) can be used to appraise the performance of the ANN model by Eq. (9)

$$MSE = \frac{1}{n}\sum_{i=1}^{n}(Y_i - Y_i^{'})^2 \tag{9}$$

In this equation, n is the number of samples in the training or testing data; Yi is the desired (measured) output;

Table 3 The optimum network parameters

Parameter	Value
Number of training data	52
Number of testing data	52
Maximum epoch number	1000
Learning rate (l_r)	0.2
Momentum constants	0.3
ANN structure	7:HN:1
Number of hidden neurons (best)	10
R^2 (training)	0.992
R^2 (testing)	0.969

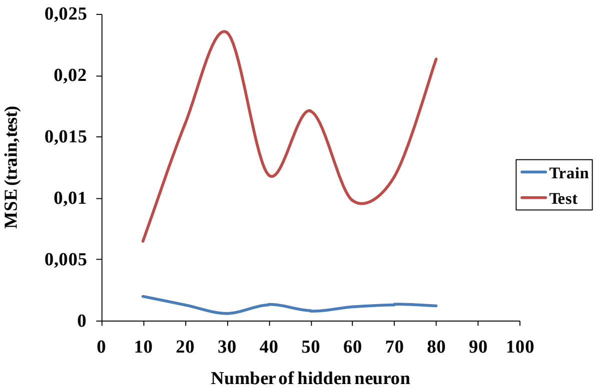

Fig. 3 Training and testing errors versus the number of hidden layer neurons

and *Yi'* is the estimated output of the neural networks. In this study, the training and testing errors versus the number of hidden layer neurons were computed for the training and testing phases (Fig. 3).

The performance values for the GDX back-propagation method related to the determination of the shear strength of FRP-RC beams are presented in Table 3. Also, performance of ANN for train and test stage is shown in Fig. 4. A general examination is available for the success of the developed ANN model:

• Selecting a different number of hidden nodes (HN) between 10 and 100 for the hidden layer, an optimum number of nodes was determined by applying separate solutions for each node. Fixing the number of nodes of the hidden layer requires multiple trials. The most important factor affecting the success of the application (except for the number of hidden layer neurons, iteration number, learning rate, momentum constant and error tolerance parameters given in Table 3) is the learning algorithm. Each parameter affects the performance during the solution of the problem because of their different properties. The determination of the function type appropriate to the behavior of the problem can change the percentage of success.

• The back-propagation method obtained a 96.9% averaged accuracy rate (100%-error%) in the test phase of the neural network. The training phase of the related algorithm is very high (R^2=0.992).

• Because this study is not a “real time” application, the training time should not be considered as a significant performance property.

• The selection of the data used in the training set and algorithm directly influences the accuracy and rate. Therefore, the selection of the algorithm most appropriate for each data set is a crucial factor in the solution of the problem.

• The success of the ANN training algorithm depends on the data set and the structure of the network. The selected ANN model presented above is valid only for the ranges for the database given in Table Appendix.

5.2 Building code(ACI440.1R-15, JSCE) and Existing Literature (EL) results

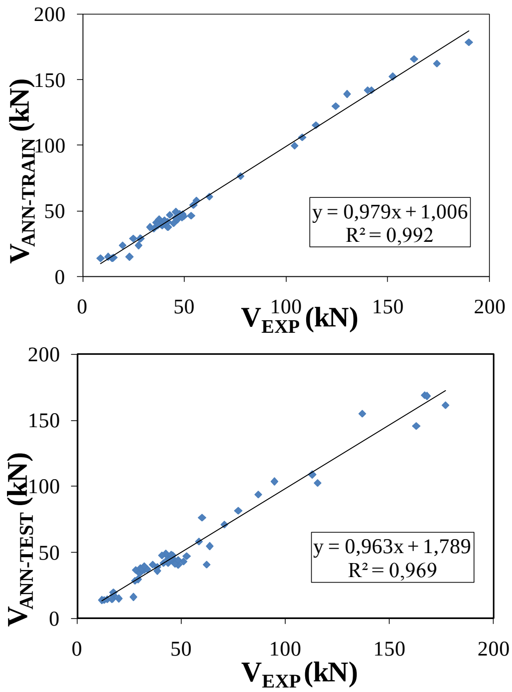

Fig. 4 Performance of ANN for train and test stages

To investigate the precision of the current standards for the shear strength of FRP-RC beams, the test results given in Table Appendix were compared with the other conventional (EL) and code approaches from selected building codes (ACI440.1R-15 (2015) and JSCE (1997). The predicting capability of the codes and EL related to the shear strength of the 104 FRP-RC members is presented in Fig. 5 and Table 4. From Fig. 5, ACI440.1R-15 has the closest estimating capacity when compared to the JSCE code and EL for the shear strength of beams in terms of R^2 values.

5.3 Comparison of the ANN model with building code equations and EL

The shear capacities of the FRP-RC beams estimated by the proposed ANN model and the predictions of the conventional approaches explained in Section 2 were compared with the compiled experimental database in Table Appendix. From Table 4, the algorithm displayed better estimates than the other conventional (EL) and current code approaches (ACI440.1R-15 and JSCE) when comparing the correlation coefficient (R^2). The proposed ANN model predicted the shear capacities of FRP-RC beams with approximately 96.9 % accuracy. The proposed ANN model and the ACI440.1R-15 results were the most similar according to R^2 values. The estimation capacities of the conventional approaches were slightly lower than those obtained by the ANN approach for R^2. In Figs. 4 and 5, a comparison of the experimental (measured) and estimated (simulated) shear strengths is shown.

Additionally, the mean squared error (MSE), root mean squared error (RMSE), mean absolute error (MAE) and mean absolute percentage error (MAPE) performance parameters were then used to appraise the performance of

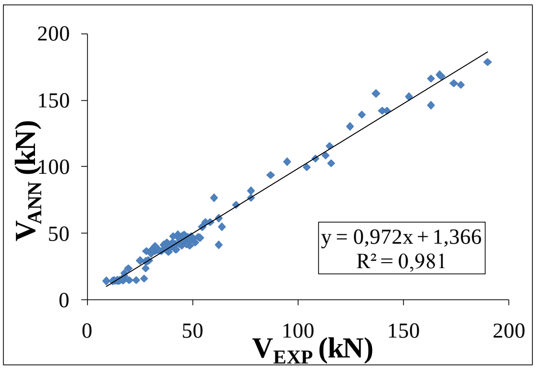

(a) ANN-entire data (test and train)

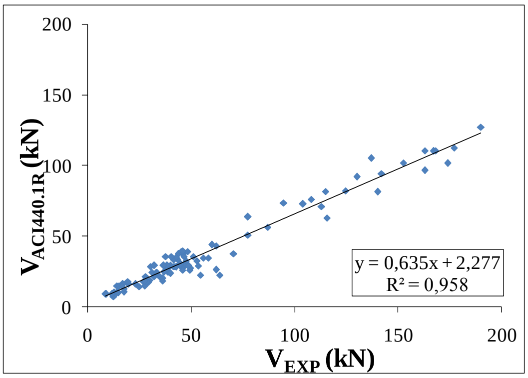

(b) ACI440.1R

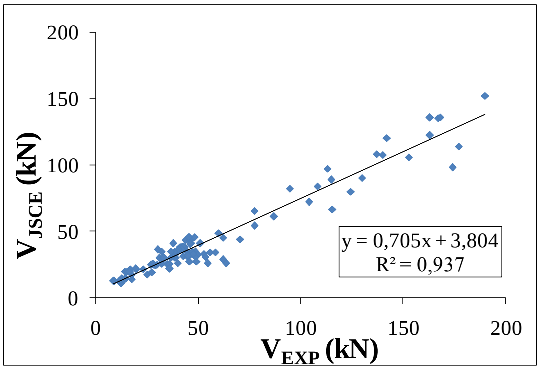

(c) JSCE

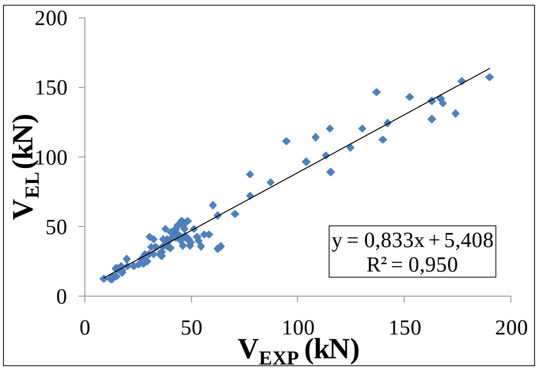

(d) EL

Fig. 5 Performance of ANN, code approaches and EL when estimating the shear strength capacity of beams in terms of R^2

the methods. The MSE, RMSE, MAE and MAPE performance parameters were computed by Eqs. (9), (10), (11) and (12), respectively.

$$RMSE = \sqrt{\frac{1}{n}\sum_{i=1}^{n}(Y_i - Y_i^{'})^2} \tag{10}$$

$$MAE = \frac{1}{n}\sum_{i=1}^{n}\left|Y_i - Y_i^{'}\right| \tag{11}$$

$$MAPE = \frac{1}{n}\sum_{i=1}^{n}\left|\frac{Y_i - Y_i^{'}}{Y_i}\right| \tag{12}$$

In the above equations, n is the number of samples in the training or testing data; Y_i is the desired output (measured values); and Y_i' is the estimated output of the neural networks and other methods (simulated values of the ANN, EL and code approaches). The performance parameters for the applied methods are shown in Table 4. From Table 4, the ANN model displayed the best performance when analyzing the R^2, MSE, RMSE, MAE and MAPE parameters. In this study, additionally, the coefficient of efficiency (E), also called Nash Sutcliffe coefficient (NSC) (Nash and Sutcliffe 1970, Grunwald and Frede 1999) was determined by what analysis tool. This is used to measure the fit between the predicted (estimated) and measured values. The Nash Sutcliffe coefficient (E) for the estimated and measured values can be computed as Eq. (13).

$$E = \frac{\sum_{i=1}^{n}(Y_i - Y_{iea\_avg})^2 - \sum_{i=1}^{n}(Y_i - Y_i^{'})^2}{\sum_{i=1}^{n}(Y_i - Y_{iea\_avg})^2} \qquad i = 1,2,\ldots.n \tag{13}$$

In this formula, E is the coefficient of efficiency (Nash Sutcliffe coefficient), Y_i is the measured value, Y_i' is the estimated value and Y_{iea_avg} is arithmetic average measured value. The best NSC parameter was obtained for ANN model according to Table 4 and Fig. 6.

According to Table 4, the ANN model exhibits a reasonably good performance when determining the shear capacities of FRP-RC beams. In Fig. 6, comparisons of estimated (simulated) data and experimental (measured) data for all considering performance parameters are shown. Although very high R^2 values had been obtained for ACI440.1R-15 and JSCE codes, lower performance values were found for other performance parameters when comparing with other methods (Table 4 and Fig. 6). However the similar results were obtained by ANN model and EL method for R^2 and NSC parameters. Also, the best performance was obtained by ANN method for all performance parameters.

A theoretical line for $V_{r(calculated)}/V_{r(experimental)}$ =1 is also drawn on the figures to display the overall trend. Figs. 7 and 8 show the errors which are induced by the discrepancy of $\sqrt{f_c'}.b_w.d'$, a/d, ρ_f, $\rho_f.E_f$ between the test specimens and the ANN model, ACI440.1R-15, JSCE codes and EL. Wide ranges of parameters are effective for determining the strength behavior of FRP reinforced concrete beams; therefore, all selected parameters should be considered. In this study, several parameters were grouped to understand the effects.

Accordingly, Figs. 7 (a) and 8 (a) show the contribution

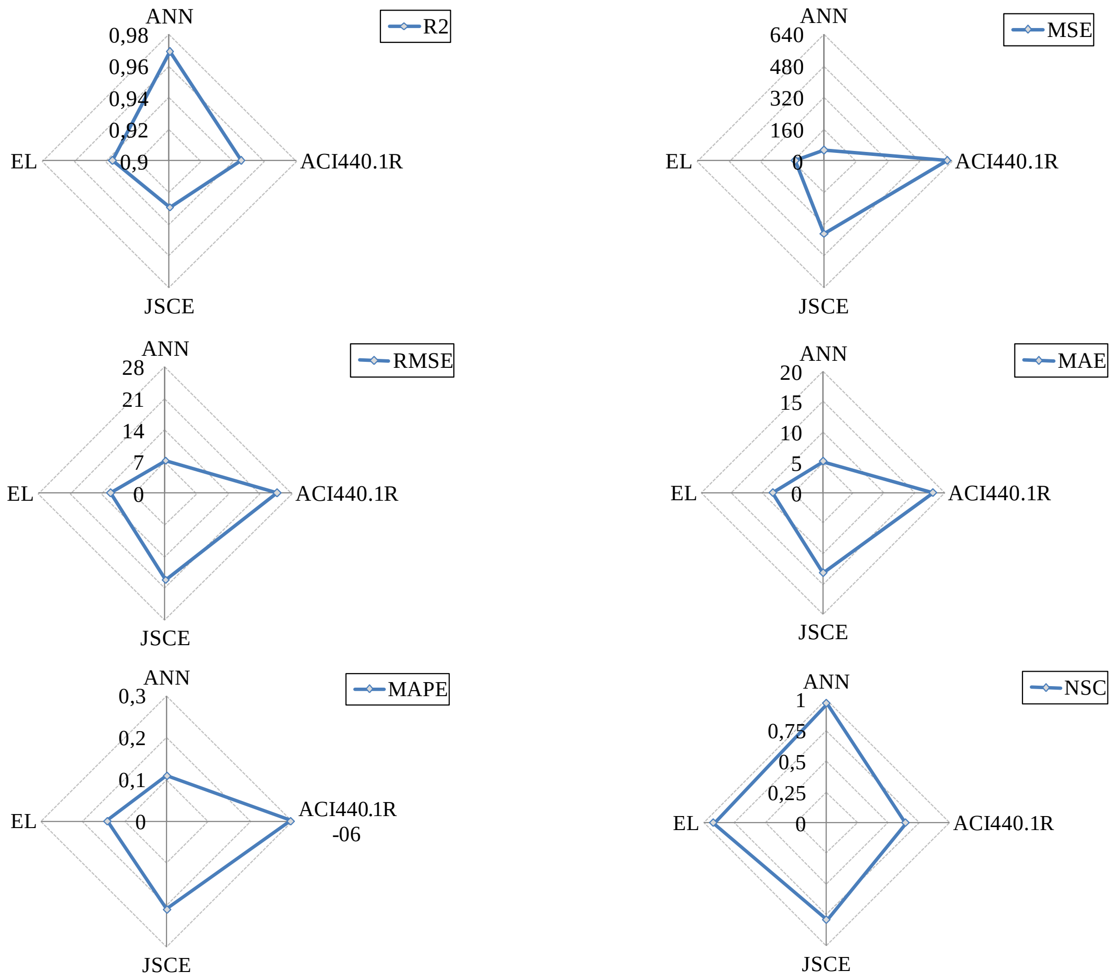

Fig. 6 Comparison of estimated (simulated) data and experimental(measured) data in terms of R^2, MSE, RMSE, MAE, MAPE and NSC for test data

Table 4 Performance results of the prediction methods

Prediction methods	Performance parameters					
	R^2	MSE	RMSE	MAE	MAPE	NSC
ANN-train	0.992	16.7876	4.0973	3.0900	0.0846	0.992
ANN-test*	0.969	53.3467	7.3039	5.1817	0.1080	0.969
ACI440. 1R-15*	0.945	615.335	24.80595	18.14759	0.29495	0.642
JSCE*	0.929	365.862	19.12752	13.18623	0.210095	0.787
EL*	0.936	145.3235	12.05502	8.321747	0.142408	0.916
ACI440. 1R-15	0.958	635.9646	25.2183	18.6966	0.2992	0.665
JSCE	0.937	400.5138	20.0128	13.8895	0.2182	0.787
EL	0.950	138.7088	11.7775	8.0384	0.1383	0.927

Note: *Performance values were computed for the test stage results of the model, and the other code values were computed for all test data.

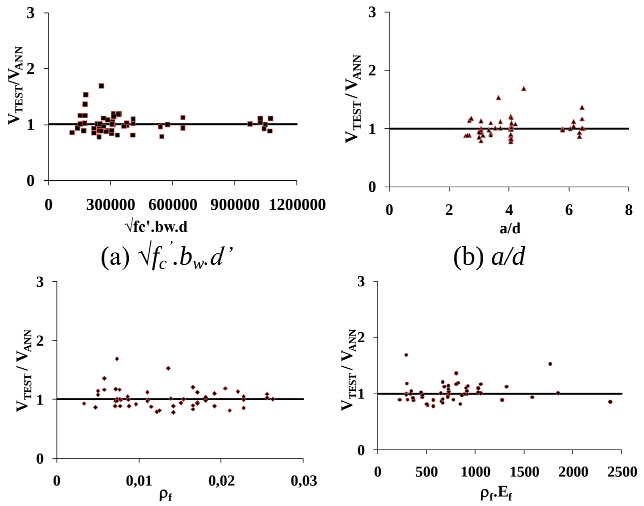

(a) $\sqrt{f_c^{'}}.b_w.d$' (b) *a/d*

(c) ρ_f (d) $\rho_f.E_f$

Fig. 7 Effect of the parameters "$\sqrt{f_c^{'}}.b_w.d$", "*a/d*", "ρ_f" and "$\rho_f.E_f$" on the shear strength of the FRP-RC beams according to ANN test values

of the concrete within the effective section of a beam to the shear strength capacity; in the figures, $\sqrt{f_c'}.b_w.d$ was used. According to the building codes, $\sqrt{f_c'}.b_w.d$ is a function of the diagonal crack strength.

Figs. 7 (b) and 8 (b) display the effect of *a/d* on the behavior of the beam; *a/d* is the shear span to effective depth ratio that plays an important role in the shear failure type and cracking pattern. The mechanical characteristics of

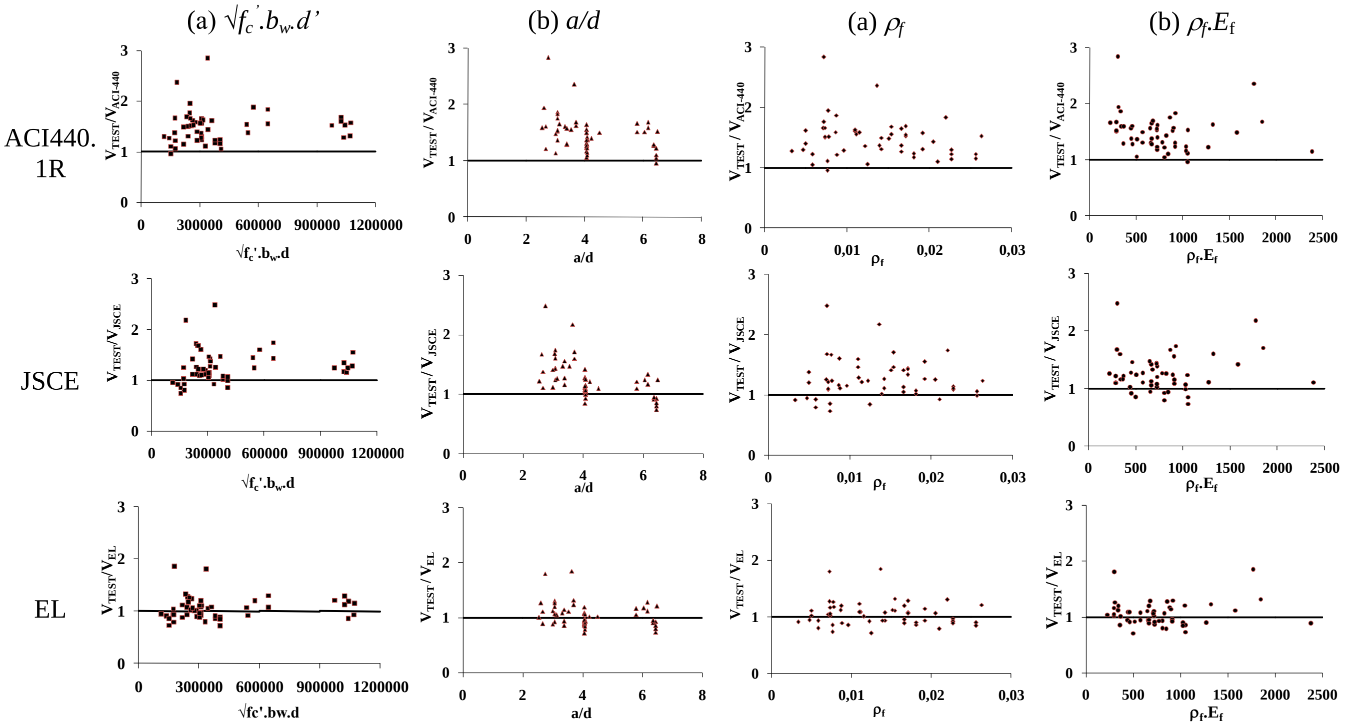

Fig. 8 Effect of the parameters "$\sqrt{f_c'}.b_w.d$", "*a/d*", "ρ_f" and "$\rho_f.E_f$" on the shear strength of the FRP-RC beams according to ACI440.1R, JSCE codes and EL

the internal FRP used for longitudinal reinforcement are among the major factors that govern the strength of FRP-RC member. Therefore, the effect of fiber reinforced polymer reinforcements on the shear strength is calculated using ρ_f and $\rho.E_f$. The FRP effect on the shear strength of FRP-RC beams is calculated using identical equations in the building codes. Figs. 7(c), (d) and 8(c), (d) display the relationship between parameters.

According to Figs. 7 and 8, ACI440.1R-15 and JSCE codes were found more conservative than ANN and EL methods for estimating the shear strength of FRP-RC beams as expected.

6. Conclusions

In this paper, an ANN model was developed to estimate the shear strength of FRP-reinforced concrete beams without stirrups. To analyze the performance of the proposed ANN model, 104 different RC specimen tests that were collected from the literature by Kara (2011) were used in the testing and training stages of the ANN. Additionally, the success of the proposed ANN method was compared to several current code approaches. The following conclusions are drawn from the results presented:

• The results obtained from the testing/training dataset of the proposed ANN model were satisfactory (the accuracy rate was calculated as ≈97 %). The predictions of the proposed ANN model better represent the experimental data than those of the other considered methods.

• Current building codes are slightly more limited in predicting the shear strength of RC beams reinforced by internal FRP reinforcement without stirrups than the ANN model in terms of R^2.

• Although in ACI440.1R-15 and JSCE codes very highest value for R^2 was obtained, the similar values were not obtained in other performance parameters. In all MSE, RMSE, MAE, MAPE and NSC performance parameters, the best values were obtained in ANN model. Although R^2 values which obtained from ACI440.1R-15 and JSCE codes were very highest values, in other performance parameters the obtained values were not satisfied the R^2 values. Particularly, ignored parameters in the current codes also affect the shear strength.

• In the present study, a similar dataset was used as investigated in Kara (2011). In this study, however, an ANN model was mainly used to determine the shear strength of the FRP-RC beams. Therefore, the obtained accuracy rate is different from the above study.

• The appropriateness of the algorithm and the data set used in the training phase directly affects the accuracy and speed of the test results. To provide an estimate, the selection of the algorithm appropriate to the data set is as significant parameter as the optimum hidden nodes, iteration number (training cycles), learning rate, momentum constant and error tolerance.

• The performance of the proposed ANN model was limited to the range of the input data used in the training and testing processes. The model can easily be further developed with additional new data. To increase the accuracy of the model and to accommodate a mechanical basis, additional studies are required to verify the applicability of the proposed model over a wider range of geometric and material parameters.

• According to the current codes, the concrete contribution to the shear strength in the beams V_c is a function of the concrete strength, the volumetric ratio of the main flexural reinforcement, the shear span-depth ratio and the member size.

• The existing ACI440.1R-15 code method is highly conservative. This code assumes a linear relationship between V_c and $E_f \cdot \rho_f$ and the resulting predicted values were obtained different from the corresponding experimental results. Additionally, the most conservative shear strength values were determined when using the ACI440.1R-15 and JSCE codes.

References

ACI440.1.R-15 (2015), Guide for the Design and Construction of Structural Concrete Reinforced with Fiber-Reinforced Polymer (FRP) Bars, American Concrete Institute, Farmington Hills, MI.

Alkhrdaji, T., Wideman, M., Belarbi, A. and Nanni, A. (2001), "Shear strength of GFRP RC beams and slabs", *Proceedings of the International Conference, Composites in Construction*, Porto, Portugal.

Arslan, C. (2013), "Improved un-gauged streamflow prediction using three artificial neural networks methods for LeeserZab", *IRECE, Int. Rev. Civil Eng.*, **4**(5), 277-283.

Arslan, M.H. (2010), "An evaluation of effective design parameters on earthquake performance of RC buildings using neural networks", *Eng. Struct.*, **32**(7), 1888-1898.

Ashour, A.F. (2006), "Flexural and shear capacities of concrete beams reinforced with GFPR bars", *Constr. Build. Mater.*, **20**, 1005-1015.

Bank, L.C. and Shapira, A. (1997), "Structural and construction aspects of novel multidimensional reinforcements for concrete", *Proceedings of the 3rd International Symposium on Non-Metallic (FRP) Reinforcement for Concrete Structures (FRPRCS-3)*, Japan Concrete Inst., Tokyo, Japan.

Bousselham, A. and Chaallal, O. (2006), "Behavior of reinforced concrete T-beams strengthened in shear with carbon fiber-reinforced polymer-an experimental study", *ACI Struct. J.*, **103**(3), 339-347.

Buyukyildiz, M., Tezel, G. and Yılmaz, V. (2014), "Estimation of the change in lake water level by artificial intelligence methods", *Water Res. Manage.*, **28**(13), 4747-4763.

CNR-DT 203/2006 (2007), Guide for the Design and Construction of Concrete Structures Reinforced with Fiber-Reinforced Polymer Bars, Italian National Research Council, Rome, June.

Costa, I.G. and Barros, J.A.O. (2010), "Flexural and shear strengthening of RC beams with composite materials-The influence of cutting steel stirrups to install CFRP strips", *Cement Concrete Compos.*, **32**, 544-553.

CSA 2002 (2007), Design and Construction of Building Components with Fibre-Reinforced Polymers, CSA-S806-02 (R2007), Canadian Standards Association (CSA) International, Toronto, Canada.

Deitz, D.H., Harik, I.E. and Gesund, H. (1999), "One-way slabs reinforced with glass fiber reinforced polymer reinforcing bars", *Proceedings of the 4th International Symposium, Fiber Reinforced Polymer Reinforcement for Reinforced Concrete Structures*, MI, 279-286.

Duranovic, N., Pilakoutas, K. and Waldron, P. (1997), "Tests on concrete beams reinforced with glass fibre reinforced plastic bars", *Proceedings of the 3rd International Symposium on Non-metallic (FRP) Reinforcement for Concrete Structures (FRPRCS-3)*, Japan Concrete Inst., **2**, Sapporo, Japan.

Elkordy, M.F., Chang, K.C. and Lee, G.C. (1993), "Neural networks trained by analytically simulated damage states", *J. Comput. Civil Eng.*, **7**(2), 130-145.

El-Sayed, A.K., El-Salakawy, E.F. and Benmokrane, B. (2006), "Shear strength of FRP-reinforced concrete beams without transverse reinforcement", *ACI Struct. J.*, **103**(2), 235-243.

El-Sayed, A.K., El-Salakawy, E.F. and Benmokrane, B. (2006), "Shear capacity of high-strength concrete beams reinforced with fiber-reinforced polymer bars", *ACI Struct. J.*, **103**(3), 383-389.

fib Bulletin No. 40 (2007), FRP Reinforcement in RC Structures.

Fu, L. (1994), *Neural Networks in Computer Intelligence*, McGraw-Hill, USA.

Gross, S.P., Dinehart, D.W., Yost, J.R. and Theisz, P.M. (2004), "Experimental tests of high-strength concrete beams reinforced with CFRP bars", *Proceedings of the 4th International Conference on Advanced Composite Materials in Bridges and Structures (ACMBS-4)*, Calgary, Alberta, Canada, July.

Gross, S.P., Yost, J.R., Dinehart, D.W., Svensen, E. and Liu, N. (2003), "Shear strength of normal and high strength concrete beams reinforced with GFRP reinforcing bars", *Proceedings of the International Conference on High Performance Materials in Bridges*, ASCE, 426-437.

Grunwald, S. and Frede, H.G. (1999), "Using the modified agricultural non-point source pollution model in German watershed", *Catena*, **37**, 319-328.

Hadi, M.N.S. (2003), "Neural network applications in concrete structures", *Comput. Struct.*, **81**, 373-381.

Inel, M. (2007), "Modeling ultimate deformation capacity of RC columns using artificial neural networks", *Eng. Struct.*, **29**(3), 329-335.

ISIS Design Manual No. 3 (2007), Reinforcing Concrete Structures with Fibre Reinforced Polymers (FRPs), ISIS Canada.

JSCE (1997), Recommendation for Design and Construction of Concrete Structures using Continuous Fiber Reinforcing Materials, Concrete Engineering Series 23, Japan Society of Civil Eng.,Tokyo, Japan.

Ju, M., Park, C. and Kim, Y. (2017), "Flexural behavior and a modified prediction of deflection of concrete beam reinforced with a ribbed GFRP bars", *Comput. Concrete*, **19**(6), 631-639.

Kara, İ.F. (2011), "Prediction of shear strength of FRP-reinforced concrete beams without stirrups based on genetic programming", *Adv. Eng. Softw.*, **42**(6), 295-304.

Lautour, O.R. and Omenzetter, P. (2009), "Prediction of seismic-induced structural damage using artificial neural networks", *Eng. Struct.*, **31**, 600-606.

MATLAB (2006), Matrix Laboratory, Neural Network Toolbox User Guide.

Mizukawa, Y., Sato, Y., Ueda, T. and Kakuta, Y. (1997), "A study on shear fatigue behavior of concrete beams with FRP rods", *Proceedings of the 3rd International Symposium on Non-metallic (FRP) Reinforcement for Concrete Structures (FRPRCS-3)*, **2**, Japan Concrete Inst. Sapporo, Japan.

Nash, J.E. and Sutcliffe, J.V. (1970), "River flow forecasting through conceptual models Part I-A discussion of principles", *J. Hydrol.*, **10**, 282-290.

Razaqpur, A.G., Isgor, B.O., Greenaway, S. and Selley, A. (2004), "Concrete contribution to the shear resistance of fiber reinforced polymer reinforced concrete members", *ASCE J. Compos. Constr.*, **8**(5), 452-460.

Rizkalla, S., Hassan, T. and Hassan, N. (2003), "Design recommendations for the use of FRP for reinforcement and strengthening of concrete structures", *Prog. Struct. Eng. Mater.-Concrete Constr.*, **1**(5), 16-28.

Rumelhart, D.E., Hinton, G.E. and Williams, R.J. (1986), "Learning representations by back-propagating errors", *Nature*, **323**, 533-536.

Swamy, N. and Aburawi, M. (1997), "Structural implications of using GFRP bars as concrete reinforcement", *Proceedings of the 3rd International Symposium on Nonmetallic (FRP) Reinforcement for Concrete Structures (FRPRCS-3)*, **2**, Japan Concrete Institute, Sapporo, Japan.
Tariq, M. and Newhook, J.P. (2003), "Shear testing of FRP reinforced concrete without transverse reinforcement", *Proceedings of CSCE 2003-Annual Conference*, Moncton, NB, Canada.
Tezel, G. and Buyukyildiz, M. (2015), "Monthly evaporation forecasting using artificial neural networks and support vector machines", *Theor. Appl. Climatol*, **124**(1-2), 69-80.
Tureyen, A.K. and Frosch, R.J. (2002), "Shear tests of FRP-reinforced concrete beams without stirrups", *ACI Struct. J.*, **99**(4), 427-434.
Tureyen, A.K. and Frosch, R.J. (2003), "Concrete shear strength: another perspective", *ACI Struct. J.*, **100**(5), 609-615.
What: *Web-based Hydrograph Analysis Tool*, https://engineering.purdue.edu/~what/
Yavuz, G. (2016), "Shear strength estimation of RC deep beams using the ANN and strut-and-tie approaches", *Struct. Eng. Mech.*, **57**(4), 657-680.
Yavuz, G., Arslan, M.H. and Baykan, O.K. (2014), "Shear strength predicting of FRP-strengthened RC beams by using artificial neural networks", *Sci. Eng. Compos. Mater.*, **21**(2), 239-255.
Yost, J.R., Gross, S.P. and Dinehart D.W. (2001), "Shear strength of normal strength concrete beams reinforced with deformed GFRP bars", *J. Compos. Constr.*, **5**(4), 268-275.
Zhao, W., Mayama, K. and Suzuki, H. (1995), "Shear behaviour of concrete beams reinforced by FRP rods as longitudinal and shear reinforcement", *Proceedings of the 2nd International Rilem Symposium on Non-metallic (FRP) Reinforcement for Concrete Structures (FRPRCS-2)*, Ghent, Belgium.

CC

Notations

a : the shear span
a/d : the aspect ratio
A_f : the area of FRP longitudinal reinforcement
b_w : the width of the beam web
c : the cracked transformed section neutral axis depth
d : the effective depth
E_f : the FRP elastic modulus
E_s : the steel elastic modulus
fc' : the concrete compressive strength
n_f : the modular ratio
V_{cf} : the shear strength
V_c : the concrete shear capacity
$V_{Rd,ct}$: the concrete contribution to shear capacity
$V_{Rd,\max}$: the concrete contribution corresponding to the shear failure because of the crushing of the web
ρ_f, ρ_l : the volumetric ratio of longitudinal FRP reinforcement
τ_{rd} : the defined design shear stress

Table Appendix. Experimental database for FRP-RC beams (Kara 2011)

Reference	f_c'(Mpa)	b_w(mm)	d (mm)	a (mm)	ρ_f (%)	E_f(Gpa)	a/d	V_{exp}(kN)
Yost *et al.* (2001)	36.3	229	225	914	1.11	40.30	4.06	39.10
	36.3	229	225	914	1.11	40.30	4.06	38.50
	36.3	229	225	914	1.11	40.30	4.06	36.80
	36.3	178	225	914	1.42	40.30	4.06	28.10
	36.3	178	225	914	1.42	40.30	4.06	35.00
	36.3	178	225	914	1.42	40.30	4.06	32.10
	36.3	229	225	914	1.66	40.30	4.06	40.00
	36.3	229	225	914	1.66	40.30	4.06	48.60
	36.3	229	225	914	1.66	40.30	4.06	44.70
	36.3	279	225	914	1.81	40.30	4.06	43.80
	36.3	279	225	914	1.81	40.30	4.06	45.90
	36.3	279	225	914	1.81	40.30	4.06	46.10
	36.3	254	224	914	2.05	40.30	4.08	37.70
	36.3	254	224	914	2.05	40.30	4.08	51.00
	36.3	254	224	914	2.05	40.30	4.08	46.60
	36.3	229	224	914	2.27	40.30	4.08	43.50
	36.3	229	224	914	2.27	40.30	4.08	41.80
	36.3	229	224	914	2.27	40.30	4.08	41.30
El-Sayed *et al.* (2006)	40	1000	165.3	1000	0.39	114.00	6.05	140.00
	40	1000	165.3	1000	0.78	114.00	6.05	167.00
	40	1000	160.5	1000	1.18	114.00	6.23	190.00
	40	1000	162.1	1000	0.86	40.00	6.17	113.00
	40	1000	159	1000	1.70	40.00	6.29	142.00
	40	1000	162.1	1000	1.71	40.00	6.17	163.00
	40	1000	159	1000	2.44	40.00	6.29	163.00
	40	1000	154.1	1000	2.63	40.00	6.49	168.00
	50	250	326	1000	0.87	128.00	3.07	77.50
	50	250	326	1000	0.87	39.00	3.07	70.50
	44.6	250	326	1000	1.24	134.00	3.07	104.00
	44.6	250	326	1000	1.22	42.00	3.07	60.00
	43.6	250	326	1000	1.72	134.00	3.07	124.50
	43.6	250	326	1000	1.71	42.00	3.07	77.50
Razaqpur *et al.* (2004)	40.5	200	225	600	0.25	145.00	2.67	36.10
	49	200	225	600	0.50	145.00	2.67	47.00
	40.5	200	225	600	0.63	145.00	2.67	47.20
	40.5	200	225	600	0.88	145.00	2.67	42.70
	40.5	200	225	800	0.50	145.00	3.56	49.70
	40.5	200	225	950	0.50	145.00	4.22	38.50
Ashour (2006)	28.9	150	167.5	666.67	0.45	38.00	3.98	12.50
	28.9	150	212.3	666.67	0.71	32.00	3.14	17.50
	28.9	150	263	666.67	0.86	32.00	2.53	25.00
	50.15	150	162.6	666.67	1.39	32.00	4.10	17.50
	50.15	150	213.3	666.67	1.06	32.00	3.13	27.50
	50.15	150	262.12	666.67	1.15	32.00	2.54	30.00
El-Sayed *et al.* (2006)	63	250	326	1000	1.71	135.00	3.07	130.00
	63	250	326	1000	1.71	42.00	3.07	87.00
	63	250	326	1000	2.20	135.00	3.07	174.00
	63	250	326	1000	2.20	42.00	3.07	115.50
Gross *et al.* (2004)	60.3	127	143	910	0.33	139.00	6.36	14.30
	60.3	127	143	910	0.33	139.00	6.36	12.90
	60.3	127	143	910	0.33	139.00	6.36	14.70
	61.8	159	141	910	0.58	139.00	6.45	19.80
	61.8	159	141	910	0.58	139.00	6.45	23.10
	61.8	159	141	910	0.58	139.00	6.45	17.00
	81.4	89	143	910	0.47	139.00	6.36	8.80
	81.4	89	143	910	0.47	139.00	6.36	11.70
	81.4	89	143	910	0.47	139.00	6.36	8.90
	81.4	121	141	910	0.76	139.00	6.45	14.30
	81.4	121	141	910	0.76	139.00	6.45	15.30
	81.4	121	141	910	0.76	139.00	6.45	16.60

Table Appendix. Continued

Reference	f_c'(Mpa)	b_w(mm)	d (mm)	a (mm)	ρ_f (%)	E_f(Gpa)	a/d	V_{exp}(kN)
Gross *et al*. (2003)	79.6	203	225	914	1.25	40.30	4.06	41.60
	79.6	203	225	914	1.25	40.30	4.06	30.40
	79.6	203	225	914	1.25	40.30	4.06	42.10
	79.6	152	225	914	1.66	40.30	4.06	31.00
	79.6	152	225	914	1.66	40.30	4.06	33.10
	79.6	152	225	914	1.66	40.30	4.06	33.50
	79.6	165	224	914	2.10	40.30	4.08	38.40
	79.6	165	224	914	2.10	40.30	4.08	32.20
	79.6	165	224	914	2.10	40.30	4.08	36.70
	79.6	203	224	914	2.56	40.30	4.08	48.30
	79.6	203	224	914	2.56	40.30	4.08	45.70
	79.6	203	224	914	2.56	40.30	4.08	45.20
Tariq and Newhook (2003)	37.3	160	346	951.5	0.72	42.00	2.75	54.50
	37.3	160	346	951.5	0.72	42.00	2.75	63.70
	43.2	160	346	1149	1.10	42.00	3.32	42.70
	43.2	160	346	1149	1.10	42.00	3.32	45.50
	34.1	160	325	1150.5	1.54	42.00	3.54	48.70
	34.1	160	325	1150.5	1.54	42.00	3.54	44.90
	37.3	130	310	949	0.72	120.00	3.06	49.20
	37.3	130	310	949	0.72	120.00	3.06	45.80
	43.2	130	310	1150	1.10	120.00	3.71	47.60
	43.2	130	310	1150	1.10	120.00	3.71	52.70
	34.1	130	310	1150	1.54	120.00	3.71	55.90
	34.1	130	310	1150	1.54	120.00	3.71	58.30
Tureyen and Frosch (2002)	39.7	457	360	1219.2	0.96	40.50	3.39	108.10
	39.9	457	360	1219.2	0.96	37.60	3.39	94.70
	40.3	457	360	1219.2	0.96	47.10	3.39	114.80
	42.3	457	360	1219.2	1.92	40.50	3.39	137.00
	42.5	457	360	1219.2	1.92	37.60	3.39	152.60
	42.6	457	360	1219.2	1.92	47.10	3.39	177.00
Alkhrdaji *et al*. (2001)	24.1	178	279	750	2.30	40.00	2.69	53.40
	24.1	178	287	750	0.77	40.00	2.61	36.10
	24.1	178	287	750	1.34	40.00	2.61	40.10
Deitz *et al.* (1999)	28.6	305	157.5	710	0.73	40.00	4.51	26.80
	30.1	305	157.5	913	0.73	40.00	5.80	28.30
	27	305	157.5	913	0.73	40.00	5.80	29.20
	28.2	305	157.5	913	0.73	40.00	5.80	28.50
	30.8	305	157.5	913	0.73	40.00	5.80	27.60
Mizukawa *et al.* (1997)	34.7	200	260	700	1.30	130.00	2.69	62.20
Duranovic *et al.* (1997)	32.9	150	210	766.5	1.36	130.00	3.65	62.20
Swamy and Aburawi (1997)	39	154	222	700	1.55	34.00	3.15	19.50
Zhao *et al.* (1995)	34.3	150	250	750	1.51	105.00	3.00	45.00
	34.3	150	250	750	3.02	105.00	3.00	46.00
	34.3	150	250	750	2.27	105.00	3.00	40.50